

# Crystal orientation-ordered ZnO nanorod bundles on hexagonal heads of ZnO microcones: epitaxial growth and self-attraction†

Xinhai Han,<sup>ab</sup> Guanzhong Wang,<sup>\*ab</sup> Lei Zhou<sup>c</sup> and J. G. Hou<sup>a</sup>

Received (in Cambridge, UK) 5th September 2005, Accepted 17th October 2005

First published as an Advance Article on the web 17th November 2005

DOI: 10.1039/b512259g

We demonstrate a preferential nucleation, epitaxial growth, and self-attraction of crystal orientation-ordered ZnO nanorod bundles on (0001) plane of single-crystal ZnO microcones.

Recent developments in nanoscience and nanotechnology have not only brought potential building blocks for nanoscale electronics and optoelectronics, but also offer an opportunity to study and imitate biological functions at the nanoscale.<sup>1–5</sup> The gecko has the ability to climb rapidly up smooth vertical surfaces due to hundreds of nanorod structures on its feet.<sup>6,7</sup> It will be interesting to imitate such structures and properties using nanotechnology. For example, Dhinojwala and the coauthors have reported constructing polymer surfaces with multiwalled carbon nanotube hairs, which have strong nanometer-level adhesion forces 200 times higher than those observed for gecko foot-hairs.<sup>8</sup> On the other hand, one-dimensional ZnO nanostructures have attracted special attention because of their unique properties and diverse hierarchical nanostructures.<sup>9,10</sup> The latter relies on the anisotropic structure of ZnO and variation of growth rate on different facets. The priority growth direction of the ZnO nanorods is along the *c*-axis, we thus expect epitaxial growth of ZnO nanorods on the (0001) plane of a single-crystal ZnO substrate. Recently, Gao and Wang reported the substrate atomic-termination-induced anisotropic growth of ZnO nanorods using the vapor–liquid–solid (VLS) process.<sup>11</sup> In this communication, we demonstrate a metal-catalyst-free approach to epitaxial growth of crystal orientation-ordered ZnO nanorod bundles on the hexagonal heads of single-crystal ZnO microcones. These nanorod bundles have a similar morphology to gecko foot hairs.

ZnO nanorod bundles were synthesized in a conventional furnace with a horizontal tube (diameter of 35 mm, length of 100 cm). Instead of well-known VLS growth using metal catalysts, we used a metal-catalyst-free method. One gram of zinc oxide powder (99.95%) source material was loaded in an alumina boat that was located at the center of the furnace. A ZnO microcone substrate was placed at the low-temperature zone in the tube. The substrate was 12 cm away from the source material. The ZnO microcones were prepared *via* vapor transport deposition at low

temperature (see ref. 12 for details). Before being heated, the tube was evacuated to  $\sim 10^{-3}$  Torr and kept under vacuum through the synthesizing process. No carrier gas was used. After being heated for 35 min, the tube reached the peak temperature of 1350 °C, and then the heating was turned off. The substrate was removed from the tube after the furnace had cooled down naturally to room temperature.

The morphologies of the substrate and as-synthesized products were analyzed using scanning electron microscopy (SEM) (JEOL 6700F). Fig. 1a shows that each ZnO microcone has a hexagonal head several micrometers across with a flat surface. X-ray diffraction spectra and transmission electron microscopy (TEM) studies have proved that the ZnO microcones are wurtzite structure single crystal with the growth direction along the *c*-axis.<sup>12</sup> Fig. 1b and 1c, the tilt view of the products with different magnifications, show hundreds of nanorods growing on the hexagonal head of a microcone forming a nanorod bundle. All nanorods growing on the same microcone are well-oriented and perpendicular to the (0001) plane surface of the ZnO microcone. The length of nanorods is about 5 micrometers, and the diameters are in the range  $110 \pm 10$  nm. The fact that all the nanorods have the same length and the same diameter implies they are synthesized

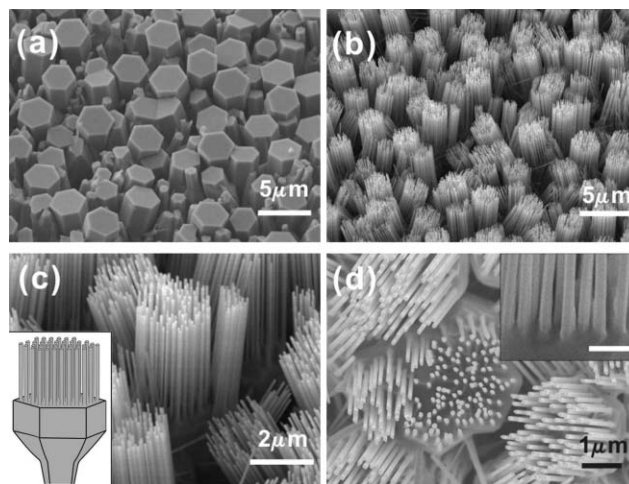


**Fig. 1** FE-SEM images of (a) tilt view of the ZnO cones substrate, (b) and (c) tilt view of ZnO nanorod bundles with different magnification. The inset in (c) is the schematic diagram of the geometry of nanorods and a microcone. (d) a top-view of a ZnO nanorod bundle. The center region of the image (d) shows that only the heads of the nanorods can be observed, indicating the very straight growth of nanorods for about 5 μm. The inset in (d) shows the root of a ZnO nanorod bundle, and the scale bar is 500 nm. All the images were obtained with the SEM accelerating voltage of 10 kV.

<sup>a</sup>Hefei National Laboratory for Physical Sciences at Microscale, University of Science and Technology of China, Hefei, Anhui, 230026, P.R. China. E-mail: gzwang@ustc.edu.cn; Fax: 86 551 3606266; Tel: 86 551 3600075

<sup>b</sup>Department of Physics, University of Science and Technology of China, Hefei, Anhui, 230026, P. R. China

<sup>c</sup>The Wallace H. Coulter Department of Biomedical Engineering, Georgia Tech/Emory University, Atlanta, Georgia, 30322, USA

† Electronic supplementary information (ESI) available: low-magnification FE-SEM images of the ZnO bundles before and after self-attraction. See DOI: 10.1039/b512259g

by the same mechanism with an equal growth rate. The inset in Fig. 1c is the schematic diagram of the morphologies. The hexagonal facet feature of the nanorods shown in the top view SEM image, Fig. 1d, provides evidence for the ZnO nanorods growing along the [0001] direction. The inset in Fig. 1d shows the adjacent edge between a bundle of nanorods and the microcone on which the nanorods grew. This image suggests an epitaxial growth of the ZnO nanorods on the ZnO microcones. Because of the single-crystal feature of the microcone and epitaxial relationship between the nanorod bundle and the substrate, the ZnO nanorod bundle is in orientation-alignment, which is further confirmed by the tip features of the nanorods, as shown in Fig. 1d.

The morphology and the microstructure of the ZnO nanorods were further investigated by TEM (JEOL 2010). Fig. 2a confirms the size uniformity of the nanorods. Fig. 2b shows the selected area electron diffraction (SAED) pattern from a nanorod, which indicates that the nanorod is single-crystal ZnO with wurtzite structure. The SAED pattern also confirms the nanorod growing along the *c*-axis, which is consistent with the SEM results. The high-resolution TEM (HRTEM) image from the head of a nanorod is shown in Fig. 2c, which presents an atomic resolved single crystal wurtzite lattice structure along the growth direction of the *c*-axis. No dislocations were observed in this area. The edges of the nanorod are clear, and no amorphous layer was observed on the surface.

Very recently, Liu's group reported ZnO hierarchical nanostructures where the ZnO hexagonal arrays of nanowires were grown on nanorods by two-step pressure-controlled vapor-reflected thermal evaporation of zinc powder at 550 °C.<sup>13</sup> They suggested that the vapor-reflected effect plays a key role in the formation of the hierarchical ZnO nanostructures. In our case, the ZnO powder was used as source material and no carrier gas was introduced into the reaction system in the fabrication of the ZnO nanorod bundles, which implies a different growth mechanism. No catalyst was used in the synthesizing process, nor were metal nanoparticles found on the heads of the nanorods, indicating that the conventional VLS process is not a suitable description for our

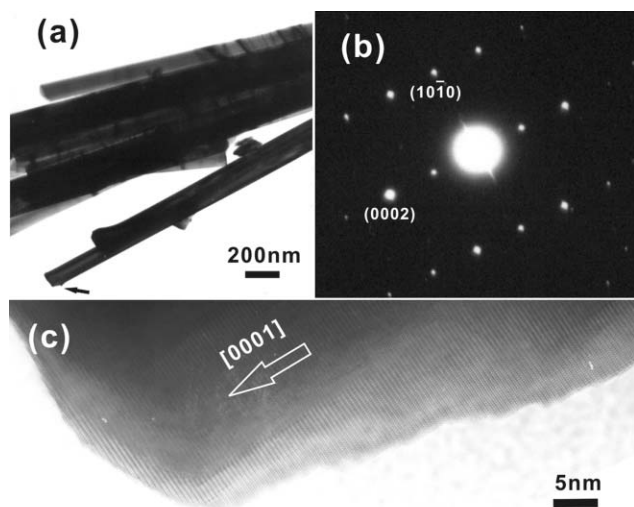


**Fig. 2** (a) A low-magnification TEM image of the ZnO nanorod bundles, and (b) the selected-area electron diffraction (SAED) pattern from the nanorod indicated by a black arrow in (a). (c) The high-resolution TEM image of the nanorod from the same spot as in (a).

case. Therefore, we suggest two factors affect the orientation of the growing uniform nanorod bundles:<sup>14</sup> First there is no carrier gas during the synthesizing process; the pressure is  $\sim 10^{-3}$  Torr during the growth. The high temperature (1250–1350 °C) and low pressure enhance the decomposition of ZnO into  $\text{Zn}^{2+}$  and  $\text{O}^{2-}$  species, and the decomposition process has been demonstrated to induce the anisotropic growth of nanobelts.<sup>15</sup> The second is the lattice-matched substrate of the ZnO microcones. The heads of the microcones in Fig. 1a seem very flat with the SEM accelerating voltage of 10 kV. However, when the accelerating voltage was changed from 10 kV to 1 kV, more details of the heads are observed, as shown in Fig. 3a. The edges of the SEM image are much sharper and are not overbright at low incident energies.<sup>16</sup> The surface of the head in Fig. 3a consists of many nanoscale raised dots. These raised dots probably supply the preferential nucleation sites for the ZnO nanorods since the density of the raised dots is close to that of the nanorods on microcones. Considering the above results, we propose a mechanism to describe the ZnO nanorod bundles growth: When the temperature of the source exceeds  $\sim 1250$  °C, sufficient  $\text{Zn}^{2+}$  and  $\text{O}^{2-}$  species are yielded due to the decomposition of the zinc oxide powder and diffuse to the substrate. The  $\text{Zn}^{2+}$  and  $\text{O}^{2-}$  species and ZnO vapor preferably nucleate on nanoscale raised dots of the surface. Continuous diffusion of  $\text{Zn}^{2+}$  and  $\text{O}^{2-}$  species and ZnO vapor to the substrate region sustains the growth of the ZnO nanorods. Single-crystal substrate may help well-aligned ZnO nanorod bundles growth. By comparison, only ZnO nanorod arrays with large diameter distribution were achieved on polycrystal ZnO thin film.<sup>14</sup> That no carrier gas was introduced into our synthesizing process also results in a steady vapor in the reaction system, which favors a stable growth of the nanorods. In contrast, the carrier gas used in the vapor transport method should give rise to vapor turbulence in the synthesizing process.

As shown in Fig. 3b, the ZnO nanorod bundles were observed to be self-attracted when they were re-examined 20 days after the first FE-SEM investigation. Recently, Wang and coauthors reported self-attraction among aligned Au/ZnO nanorods under electron beam, which is due to the interaction between the accumulated charges near the metal–semiconductor junctions for two nanorods of different length.<sup>17</sup> In our case, no metal catalyst is used and no metal nanoparticles are found on the tips of the nanorods. Therefore, the model presented by Wang is not suitable

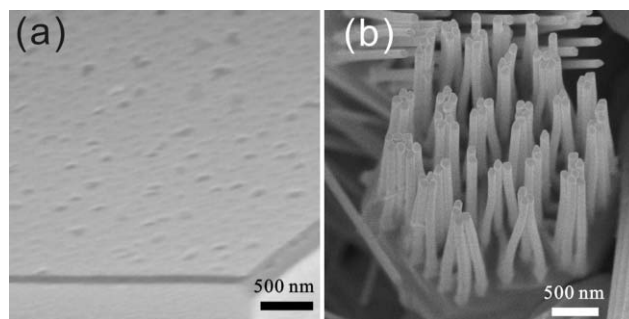


**Fig. 3** (a) FE-SEM image of the microcone head surface with accelerating voltage of 1 kV. Many nanoscale raised dots are observed on the surface of the head, which probably supply the preferential nucleation sites for the ZnO nanorods. (b) FE-SEM image of the self-attracted ZnO nanorod bundles on a hexagonal head of ZnO microcone.

for our case. The mechanism of the bending properties is under investigation.

As a unique hierarchical ZnO structure, the ZnO nanorod bundles on microcones are suggested to have potential in many device applications: First, the ZnO cones and the nanorod bundles are aligned and vertical to the silicon substrate, so the structures probably have applications as conventional ZnO nanoarrays in nanosensor,<sup>18</sup> and field emission.<sup>19</sup> Secondly, because of their unique multi-forked structure, they may be used as nanoscale optical waveguide splitters and recombiners.<sup>20–22</sup> Thirdly, in particular, the bending feature of the ZnO nanorods could be applied as nanotweezers to capture nanoparticles or other nanostructures, although the self-attraction between the ZnO nanorods is not clear yet. Furthermore, the diameter of a microcone is several micrometers and the length more than 10  $\mu\text{m}$ , which allows it to be manipulated and fixed more easily than a nanostructure. Therefore, the hierarchical ZnO structures have great advantages as nanotweezers. Fourthly, the nanorod bundles have morphology similar to a gecko's foot hairs. This structure could be used to imitate the function of a gecko's foot by adjusting the shape of the bundles.<sup>8</sup>

In conclusion, we have demonstrated a new approach to epitaxial growth of crystal orientation-ordered ZnO nanorod bundles on (0001) plane of single-crystal ZnO microcones. We suggest that the high temperature (1250–1350 °C) and low pressure ( $\sim 10^{-3}$  Torr) enhance the ZnO decomposing into  $\text{Zn}^{2+}$  and  $\text{O}^{2-}$  species, and sufficient and steady  $\text{Zn}^{2+}$  and  $\text{O}^{2-}$  vapor help nucleate at the raised dots on the heads of the microcones, and finally the well-aligned epitaxial ZnO nanorod bundles are formed on the microcones. The ZnO nanorod bundles were also observed to be self-attracted. With the bending properties, the uniform ZnO nanorod bundles could be used as nanotools.

We thank Mr Gongpu Li and Professor Fanqing Li for their assistance in TEM and SEM experiments. This work was supported by Natural Science Foundation of China (Grant No. 50121202, 60376008).

## Notes and references

- 1 X. F. Duan, Y. Huang, R. Agarwal and C. M. Lieber, *Nature*, 2003, **421**, 241.
- 2 C. Y. Geng, Y. Jiang, Y. Yao, X. M. Meng, J. A. Zapien, C. S. Lee, Y. Lifshitz and S. T. Lee, *Adv. Funct. Mater.*, 2004, **14**, 589.
- 3 Y. N. Xia, P. D. Yang, Y. G. Sun, Y. Y. Wu, B. Mayers, B. Gates, Y. D. Yin, F. Kim and Y. Q. Yan, *Adv. Mater.*, 2003, **15**, 353.
- 4 Y. Wang, Z. Y. Tang, S. S. Tan and N. A. Kotov, *Nano Lett.*, 2005, **5**, 243.
- 5 A. P. Alivisatos, *Science*, 1996, **271**, 933.
- 6 A. P. Russell, *J. Zool. Lond.*, 1975, **176**, 437.
- 7 K. Autumn, Y. A. Liang, S. T. Hsieh, W. Zesch, W. P. Chan, T. W. Kenny, R. Fearing and R. J. Full, *Nature*, 2000, **405**, 681.
- 8 B. Yurdumakan, N. R. Raravikar, P. M. Ajayan and A. Dhinojwala, *Chem. Commun.*, 2005, 3799.
- 9 Z. L. Wang, X. Y. Kong, Y. Ding, P. X. Gao, W. L. Hughes, R. S. Yang and Y. Zhang, *Adv. Funct. Mater.*, 2004, **14**, 943.
- 10 J. Y. Lao, J. Y. Huang, D. Z. Wang and Z. F. Ren, *Nano Lett.*, 2003, **3**, 235.
- 11 P. X. Gao and Z. L. Wang, *J. Phys. Chem. B*, 2004, **108**, 7534.
- 12 X. H. Han, G. Z. Wang, J. S. Jie, W. C. H. Choy, Y. Luo, T. I. Yuk and J. G. Hou, *J. Phys. Chem. B*, 2005, **109**, 2733.
- 13 R. C. Wang, C. P. Liu, J. L. Huang and S. J. Chen, *Appl. Phys. Lett.*, 2005, **86**, 251104.
- 14 X. H. Han, G. Z. Wang, Q. T. Wang, L. Cao, R. B. Liu, B. S. Zou and J. G. Hou, *Appl. Phys. Lett.*, 2005, **86**, 223106.
- 15 X. Y. Kong and Z. L. Wang, *Nano Lett.*, 2003, **3**, 1625.
- 16 *Handbook of Nanophase and Nanostructured Materials - Characterization*, ed. Z. L. Wang, Y. Liu and Z. Zhang, Kluwer Academic/Plenum Publishers, 2002.
- 17 X. D. Wang, C. J. Summers and Z. L. Wang, *Appl. Phys. Lett.*, 2005, **86**, 013111.
- 18 X. G. Wen, Y. P. Fang, Q. Pang, C. L. Yang, J. N. Wang, W. K. Ge, K. S. Wong and S. H. Yang, *J. Phys. Chem. B*, 2005, **109**, 15303.
- 19 C. J. Lee, T. J. Lee, S. C. Lyu, Y. Zhang, H. Ruh and H. J. Lee, *Appl. Phys. Lett.*, 2002, **81**, 3648.
- 20 R. M. Jenkins, J. M. Heaton, D. R. Wight, J. T. Parker, J. C. H. Birbeck, G. W. Smith and K. P. Hilton, *Appl. Phys. Lett.*, 1994, **64**, 684.
- 21 M. Law, D. J. Sirbuly, J. C. Johnson, J. Goldberger, R. J. Saykally and P. D. Yang, *Science*, 2004, **305**, 1269.
- 22 A. B. Greytak, C. J. Barrelet, Y. Li and C. M. Lieber, *Appl. Phys. Lett.*, 2005, **87**, 151103.